ISTITUTO DI ANALISI DEI SISTEMI ED INFORMATICA
CONSIGLIO NAZIONALE DELLE RICERCHE

A. Bertuzzi, M. Faretta, A. Gandolfi, C. Sinisgalli, G. Starace, G. Valoti, P. Ubezio

KINETIC HETEROGENEITY OF AN EXPERIMENTAL TUMOUR REVEALED BY BROMODEOXYURIDINE INCORPORATION AND MATHEMATICAL MODELLING

R. 529 Settembre 2000

Alessandro Bertuzzi – Istituto di Analisi dei Sistemi ed Informatica del CNR, Viale Manzoni 30 - 00185 Roma, Italy. Email : bertuzzi@iasi.rm.cnr.it.

Mario Faretta – Istituto di Ricerche Farmacologiche "Mario Negri", Via Eritrea 62 - 20157 Milano, Italy.

Alberto Gandolfi – Istituto di Analisi dei Sistemi ed Informatica del CNR, Viale Manzoni 30 - 00185 Roma, Italy. Email : gandolfi@iasi.rm.cnr.it.

Carmela Sinisgalli – Istituto di Analisi dei Sistemi ed Informatica del CNR, Viale Manzoni 30 - 00185 Roma, Italy.

Giuseppe Starace – Istituto di Medicina Sperimentale del CNR, Viale Marx 43 - 00137 Roma, Italy. Email : giuseppe@biocell.irmkant.rm.cnr.it.

Giorgio Valoti – Istituto di Ricerche Farmacologiche "Mario Negri", Via Gavazzeni 11 - 24125 Bergamo, Italy.

Paolo Ubezio – Istituto di Ricerche Farmacologiche "Mario Negri", Via Eritrea 62 - 20157 Milano, Italy. Email : ubezio@irfmn.mnegri.it.

This work was partially supported by the Progetto Strategico CNR "Metodi e Modelli Matematici nello Studio dei Fenomeni Biologici". The authors wish to thank C. Caruso for the graphical work.

ISSN: 1128–3378

Collana dei Rapporti
dell'Istituto di Analisi dei Sistemi ed Informatica, CNR

viale Manzoni 30, 00185 ROMA, Italy

tel. ++39-06-77161
fax ++39-06-7716461
email: iasi@iasi.rm.cnr.it
URL: http://www.iasi.rm.cnr.it

Abstract

In the present paper we propose a method of analysis of the cell kinetic characteristics of *in vivo* experimental tumours, that uses DNA-BrdUrd flow cytometry data at various times after the BrdUrd injection and mathematical modelling. The model of the cell population takes into account the cell-to-cell heterogeneity of the progression rate across cell cycle phases within the tumour, and assumes a strict correlation between the durations of S and G2M phases. The model also allows for a nonconstant DNA synthesis rate across S phase. In addition, the measurement process is modeled, considering the possibility of nonimpulsive labelling and providing a representation of the time course of the bivariate DNA-BrdUrd fluorescence distribution. Sequential DNA-BrdUrd distributions were obtained from a human ovarian carcinoma transplanted in mice. From these data, that included the fractional density and the mean BrdUrd-fluorescence of BrdUrd-positive cells as a function of the DNA-fluorescence, kinetic parameters such as the potential doubling time (T_{pot}) and the mean and variance of the transit times in S and G2M phases, were estimated. This study revealed the presence of a substantial heterogeneity in S and G2M phases within the cell population. Moreover, our analysis suggests a nonnegligible effect of the BrdUrd pharmacokinetics in the *in vivo* cell labelling.

Key words: Cell kinetics, age-structured populations, DNA-BrdUrd flow cytometry, experimental tumours.

1. Introduction

Growing cell populations are characterized by the variability of the proliferative pattern. In particular, the cell cycle duration and the residence times in the different cycle phases can vary even within a genetically homogeneous population that grows in an homogeneous environment, such as an *in vitro* culture. Direct evidence of this variability was provided by *in vitro* time-lapse cinematography (Sisken and Morasca, 1965) or, indirectly, by its effects on the progression of a labelled subpopulation (Steel, 1977; Chiorino *et al.*, 2001). The technique based on cell labelling by a radioactive DNA precursor and subsequent autoradiography evidenced a wider variability occurring in the *in vivo* growing populations, such as in the experimental and spontaneous tumours (see Steel, 1977, for a comprehensive review of these results). This is not surprising since the concentration of oxygen and nutrients in tumours can be quite heterogeneous (Kallinowski *et al.*, 1989) and because of the possible presence of different phenotypes with different kinetic characteristics (Bergers *et al.*, 1996).

The current method for assessing the kinetics of proliferating cell populations is based on the incorporation of the label bromodeoxyuridine (BrdUrd) followed by flow cytometry (Gratzner, 1982; Dolbeare *et al.*, 1983; Dolbeare, 1995). By means of this technique, that has replaced the ^{3}H-thymidine incorporation method and the autoradiography, it is possible to follow the time course of the BrdUrd-labelled (and of the unlabelled) subpopulations as related to their DNA content.

Mathematical expressions for observable quantities related to the evolution of DNA-BrdUrd histograms have been derived by assuming that there is no cell-to-cell variability of the transit times in S and G2M phases (White and Meistrich, 1986; White *et al.*, 1990; Bertuzzi *et al.*, 1995a; Bertuzzi *et al.*, 1997). The *in vivo* cell kinetics of experimental tumours has been studied under this assumption (Carlton *et al.*, 1991; Terry *et al.*, 1997; White *et al.*, 2000), but a more refined approach is advisable in view of the proliferative heterogeneity of experimental tumours. Mathematical and simulation models that predict the evolution of DNA-BrdUrd distributions assuming independently distributed phase transit times have been developed by Yanagisawa *et al.* (1985), White (1989), Ubezio (1990), Baisch and Otto (1993), Baisch *et al.* (1995). In the last two papers, *in vivo* data have been analyzed.

In the present paper we propose a new method for quantifying the proliferative heterogeneity in tumours using BrdUrd labelling and flow cytometry. This method, that exploits more completely the information contained in the data, is applied to the study of a human ovarian tumour implanted in nude mice. The time-varying shapes of the DNA distribution and of the mean BrdUrd-fluorescence of BrdUrd-labelled cells, together with the time course of the fractions of labelled undivided and labelled divided cells and of the relative movement, are analyzed by means of a mathematical model of the cell population that assumes cell-to-cell variability of phase transit times with tight correlation between the durations of S and G2M phases, and nonconstant rate of DNA synthesis across S phase. No specific assumption on cell progression in G1 phase is required to analyze data at time-points in which no labelled divided cell has yet entered S phase. The possibility of a non purely impulsive labelling is also taken into account. In a previous paper (Bertuzzi and Gandolfi, 1999) the cell population model has been investigated by numerical simulations.

2. Experimental procedure

2.1. Experimental protocol

Female NCr nu/nu mice were obtained from the Division of Cancer Treatment, National Cancer Institute, Animal Production Colony, Frederick, Maryland, USA and were used when 8-10 weeks old and weighing 21±2 g. The mice were housed in air-filtered laminar flow cabinets and manipulated according to aseptic procedures. Procedures involving animals and their care were conducted in conformity with the institutional guidelines that are in compliance with national and international laws and policies. The human ovarian carcinoma xenograft HOC18, was derived from a primary ovarian tumour from a 62 years old patient. It is maintained and grows subcutaneously in nude mice as previously described (Massazza *et al.*, 1989). The volumetric doubling time was 9.8±2.5 days.

In the experiments reported here, BrdUrd (50 mg/kg) was injected into the peritoneal cavity of the mice 39 days following tumour implant, with tumours weighing 300-500 mg. BrdUrd reaches the tumour and labels the DNA-sythesizing cells (Dolbeare *et al.*, 1983). The cells in S phase at the time of the BrdUrd exposure became therefore BrdUrd-labelled (BrdUrd+). At the subsequent times, these cells or their descendants remained BrdUrd+ and were definitely distinguishable from cells in G2, M and G1 phases at the initial time (BrdUrd-unlabeled cell, BrdUrd−). Three mice were sacrified at $t = 0.5$, 2, 4, 8, 14, 20 h after BrdUrd injection, the tumour was minced and the cells were suspended and fixed in 70% ethanol.

2.2. Flow cytometry

For the flow cytometric analysis according to the DNA-BrdUrd method, the fixed cells were stained with propidium iodide (PI) and anti-BrdUrd fluoresceinated antibody, as described before (Ubezio *et al.*, 1991). Briefly, each sample of ethanol-fixed cell suspension was centrifuged and incubated with 3N HCl for 20 min, to obtain partially denatured DNA. After neutralizing with 0.1M $Na_2B_4O_7$, the cell pellet was resuspended with 50 μl Tween 20, 0.5% in PBS. After that, 50 μl of bovine serum albumin 0.5% in PBS and 20 μl of anti-BrdUrd mouse monoclonal antibodies (Becton Dickinson) were added and the mixture was incubated for 60 min at room temperature. After washing with PBS, cells were incubated for 1 h with fluorescein (FITC)-conjugated F(ab')2 fragments of goat antimouse IgG (Jackson, West Grove, PA) diluted 1:50 in PBS with 0.5% Tween 20 and 1% NGS. After incubation with antibody, cells were centrifuged, resuspended in 2 μg/ml PI in PBS plus RNAse, incubated overnight and analyzed by flow cytometry with laser excitation tuned at 488 nm, using a FACSCalibur (Becton Dickinson) flow cytometer. The green fluorescence of fluorescein was detected in the 515-555 nm wavelength band and the red PI fluorescence above 630 nm. The fluorescence intensities of each cell were accumulated to form a biparametric histogram. At least 20000 cells were analyzed per sample.

The biparametric DNA-BrdUrd histograms were analyzed using the dedicated software (Cell Quest, Becton Dickinson) providing the fractions of cells in user-selected regions of interest, as shown in Fig. 1. Cells with green fluorescence above a given threshold were identified as BrdUrd+. A threshold value on the red fluorescence furtherly subdivided the BrdUrd+ region, giving a measure of the fractions of labelled undivided and labelled divided cells. Cell aggregates were previously excluded from the analysis using electronic pulse processing, based on a difference in the shape of the red fluorescence signal, and non-tumoral cells by gating on the DNA content. A minor "contaminant" of non-tumoral cells and aggregates, present in the selected region of tumour cells, does not substantially alter the results.

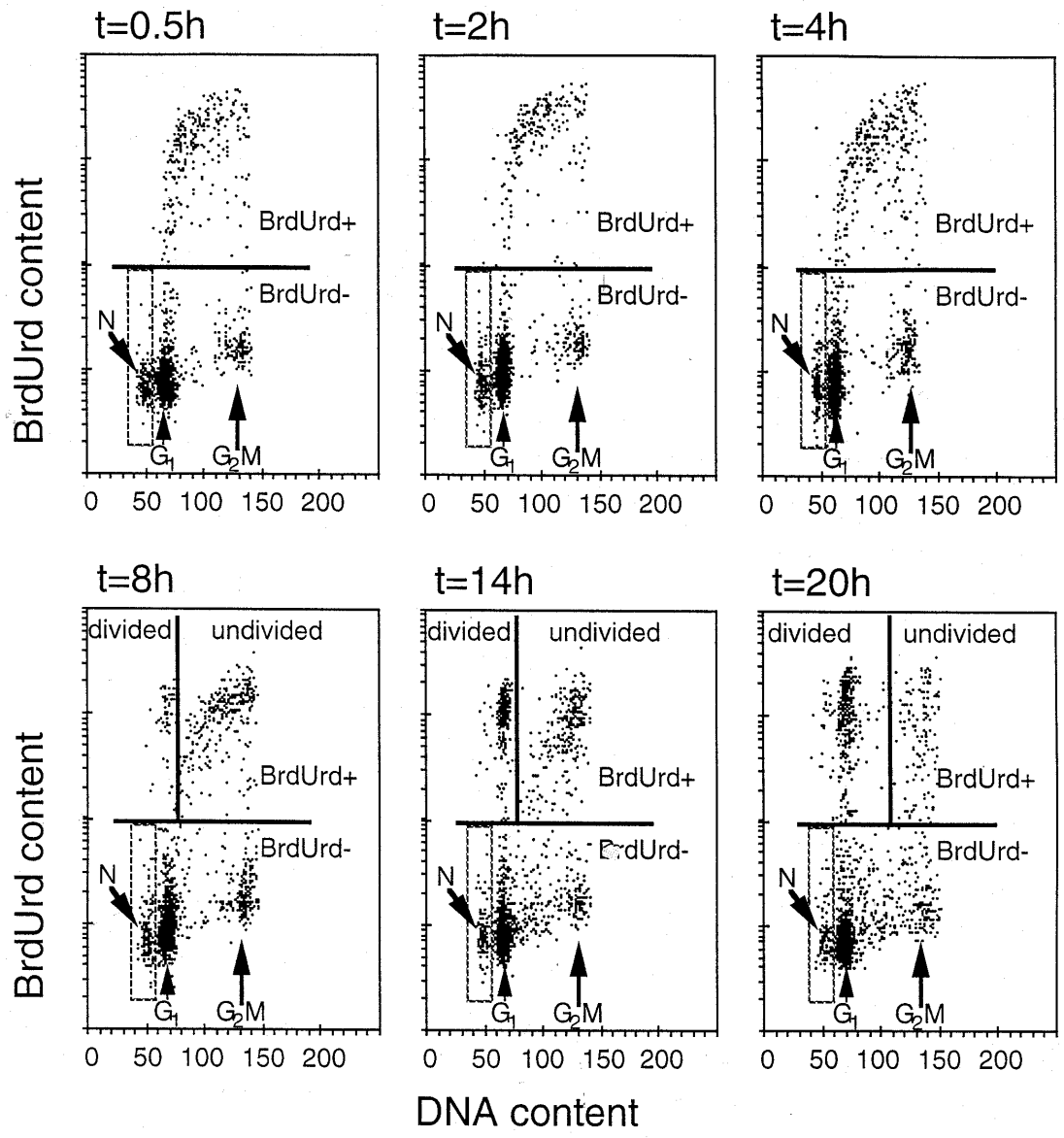

Fig. 1. Pulse-chase DNA-BrdUrd analyses at $t = 0.5$, 2, 4, 8, 14, 20 h following BrdUrd injection. Cells were considered BrdUrd-positive when detected above the line. The vertical line separates undivided (right) from divided (left) BrdUrd-positive cells. The box N contains diploid (possibly non-tumoral) cells that were excluded by gating in the subsequent data analysis. 2000 dots are shown in each plot.

The profile of BrdUrd incorporation during the S-phase was evaluated by a home-made computer program as follows. The fluorescence intensities of the tumour-BrdUrd+ cells, related to both DNA content (red fluorescence) and BrdUrd incorporation (green fluorescence), were exported as a list from the cytometer and read by the program. Then the cells were grouped in 22 windows of equal width according to the DNA fluorescence, the first centered around G1 and the last around G2M values. The percentage of cells and the mean green fluorescence intensity

were separately calculated in each window. Then, the mean green fluorescence intensity in each window was normalized to the mean fluorescence calculated by dividing the sum of the green fluorescence intensities of BrdUrd+ cells by the sum of the number of labelled undivided cells plus half the number of labelled divided cells (this normalization is motivated in section 3.4). In this way, intermouse differences of BrdUrd uptake and cell staining by monoclonal antibodies were rid of, allowing a comparison of the profiles of relative BrdUrd incorporation (and hence of DNA synthesis rate) across S-phase, but losing the information on the absolute values of the synthesis rate. In the authors' experience, the interpretation of the mean green fluorescence intensity as an absolute measure of the DNA synthesis rate, and a comparison of different samples (from independent animals, tumours, fixation, and staining procedures) for this parameter, are not correctly feasible.

3. Theory

3.1. Cell population model

A number of quantitative analyses of DNA-BrdUrd flow cytometry data (White and Meistrich, 1986; White *et al.*, 1990; Bertuzzi *et al.*, 1995) utilized a simple cell population model based on the following assumptions: (i) the cell population is in asynchronous exponential growth (AEG); (ii) there is no cell-to-cell variability in T_S and T_{G2M} (T_S and T_{G2M} denote the transit times in S and G2+M phases, respectively); (iii) no cell arrest occurs in S and G2M phases, (iv) cell loss affects all the cells of the population with a common rate constant (uniform cell loss). In this model the time spent by a newborn cell to enter S phase is not necessarily the same for all the cells of the population. Moreover, cells are allowed to decycle to a quiescent state after mitosis or from G1 phase, and cells from this resting state may reenter the cycle.

In view of a more realistic study of the *in vivo* proliferation, we proposed a cell population model in which assumption (ii) was relaxed (Bertuzzi and Gandolfi, 1999). For reader's convenience, we recall the main features of the model. The cell population is subdivided into a compartment of cells in G1 or in a quiescent state with G1 DNA content (compartment 1), and a compartment of cells in S and G2M phase (compartment 2) (see Fig. 2). Cells display different progression rates across the cycle, and we assume that the transition of cells to different progression rates only occurs after mitosis and before entry into S phase. Transitions from fast to slower progression rates are indeed required to guarantee the existence of the asynchronous exponential growth of the population, preventing the fastest cells to prevail in the growth. Compartment 2 is thus partitioned into subpopulations, each characterized by the time T required by cells to progress from entry in S to mitosis, and a cell of compartment 2 is said to be "of class T" if it belongs to such a subpopulation. Moreover, all cells of class T have transit times in S and G2M, $T_S(T)$ and $T_{G2M}(T)$ respectively, that are deterministic functions of T, with $T = T_S(T) + T_{G2M}(T)$. This assumption is consistent with the view that the different rates of progression across the cycle are mainly related to the different microenvironmental conditions experienced by the cells. Thus, a slow cell exhibiting a long S phase is likely to have a long G2M phase. Although cells arrested in S or G2M are not explicitly considered, these cells are to some degree represented by the subpopulation with the largest T. Slowly progressing cells are likely to be more susceptible to death, however for simplicity we assume a common rate constant μ of cell loss in the population.

To write down the model equations, let us start from compartment 2. Assuming T as a continuous variable with values from T' to T'', the population of S and G2M cells is described

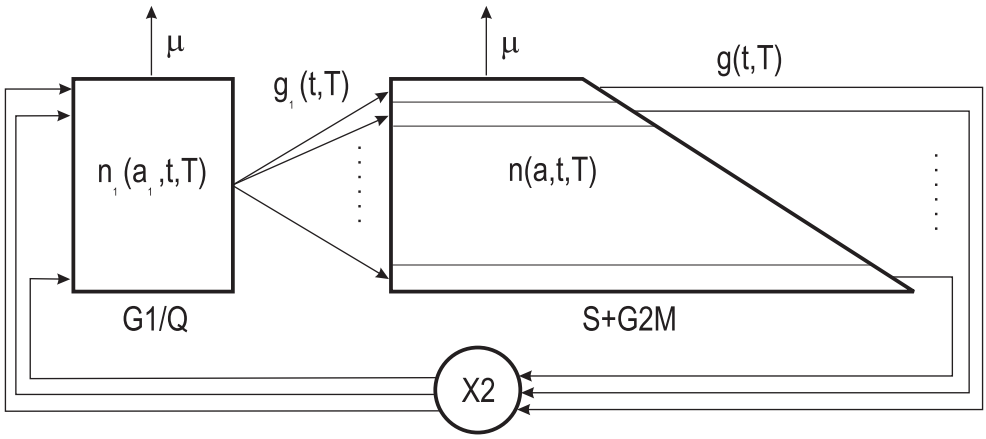

Fig. 2. Block diagram of the cell population model. Symbols are explained in the text.

by a density function $n(a,t,T)$, such that $n(a,t,T)dadT$ is the number of cells with age between a and $a+da$ at time t belonging to the subpopulation of cells that traverse S+G2M in a time length between T and $T+dT$. Age a is counted from cell entry into S phase and thus $a\in[0,T]$. For compartment 1, as will be seen in section 3.3, it is useful that cells are identified by the time class T of mother cells. Let a_1 be the age of cells in this compartment. We define thus the density $n_1(a_1,t,T)$, such that $n_1(a_1,t,T)da_1dT$ is the number of cells that have age between a_1 and a_1+da_1 at time t, and have been *generated* by cells that traversed S+G2M in a time between T and $T+dT$. If T_{1min} is the minimal time required to progress from birth to entry in S, the continuity equation for n_1 can be written for $a_1<T_{1min}$ without specifying the law of exit from compartment 1. According to the previous assumptions, $n_1(a_1,t,T)$ and $n(a,t,T)$ satisfy the continuity equations

$$\frac{\partial}{\partial t}n_1(a_1,t,T)+\frac{\partial}{\partial a_1}n_1(a_1,t,T)=-\mu n_1(a_1,t,T)\,,\quad a_1\in(0,T_{1min}) \tag{1}$$

$$\frac{\partial}{\partial t}n(a,t,T)+\frac{\partial}{\partial a}n(a,t,T)=-\mu n(a,t,T)\,,\quad a\in(0,T) \tag{2}$$

with boundary conditions

$$n_1(0,t,T)=2n(T,t,T) \tag{3}$$

$$n(0,t,T)=g_1(t,T)\,, \tag{4}$$

where $g_1(t,T)dT$ is the number of cells that leave compartment 1, to join the cells of classes between T and $T+dT$, in the unit time at time t.

In asynchronous exponential growth with growth rate α, we have $n_1(a_1,t,T)=\bar{n}_1(a_1,T)\mathrm{e}^{\alpha t}$, $n(a,t,T)=\bar{n}(a,T)\mathrm{e}^{\alpha t}$ and $g_1(t,T)=\bar{g}_1(T)\mathrm{e}^{\alpha t}$. Thus

$$n_1(a_1,t,T)=2\bar{g}_1(T)\mathrm{e}^{-\beta T}\mathrm{e}^{-\beta a_1}\mathrm{e}^{\alpha t} \tag{5}$$

$$n(a,t,T)=\bar{g}_1(T)\mathrm{e}^{-\beta a}\mathrm{e}^{\alpha t} \tag{6}$$

with $\beta=\alpha+\mu$. The mitotic rate density $g(t,T)=n(T,t,T)$, *i.e.* the density with respect to T of the number of cells undergoing division in the unit time at time t, is given by

$$g(t,T)=\bar{g}_1(T)\mathrm{e}^{-\beta T}\mathrm{e}^{\alpha t}\,. \tag{7}$$

For the cell population in AEG we can define the frequency function of T as $p_T(T) = g(t,T)/\int g(t,T)\,dT$, so we have

$$p_T(T) = \frac{\bar{g}_1(T)\mathrm{e}^{-\beta T}}{\int_{T'}^{T''} \bar{g}_1(T)\mathrm{e}^{-\beta T}\,dT}\,. \tag{8}$$

The total number of cells of the population, N, obeys the balance equation

$$\dot{N}(t) = \int_{T'}^{T''} g(t,T)\,dT - \mu N(t) \tag{9}$$

and in AEG we have $N(t)=\bar{N}\mathrm{e}^{\alpha t}$. Thus the rate constant of cell production K_p, defined as the ratio between the number of cells undergoing division in the unit time and the number of cells of the population (Steel, 1977), can be computed from (7) and (9) as:

$$K_p = \frac{1}{\bar{N}}\int_{T'}^{T''} \bar{g}_1(T)\mathrm{e}^{-\beta T}\,dT = \beta\,. \tag{10}$$

We note that K_p defines the so-called potential doubling time of the cell population, $T_{pot} = \ln 2/K_p$ (Steel, 1977). From (8) and (10) we have

$$\frac{\bar{g}_1(T)}{\bar{N}} = \beta p_T(T)\mathrm{e}^{\beta T}\,. \tag{11}$$

The fractional cell densities, $\nu_1(a_1,T)=n_1(a_1,t,T)/N(t)$ and $\nu(a,T)=n(a,t,T)/N(t)$, are thus given from (5), (6) and (11) by

$$\nu_1(a_1,T) = 2\beta p_T(T)\mathrm{e}^{-\beta a_1}\,, \quad a_1 \in [0, T_{1min}]\,, \tag{12}$$

$$\nu(a,T) = \beta p_T(T)\mathrm{e}^{\beta T}\mathrm{e}^{-\beta a}\,, \quad a \in [0,T]\,. \tag{13}$$

The fraction f_1 of cells in compartment 1 can be derived from the previous equations in terms of β and $p_T(T)$, even if the whole cell age density in compartment 1 is not described. Denoting by $N_1(t)$ the number of cells in compartment 1, we can write

$$\dot{N}_1(t) = 2\int_{T'}^{T''} g(t,T)\,dT - \int_{T'}^{T''} g_1(t,T)\,dT - \mu N_1(t)\,. \tag{14}$$

Since $N_1(t)=f_1 N(t)$ in AEG, expressing $\bar{g}_1(T)$ in terms of $p_T(T)$ by means of (8), we have

$$\beta f_1 = \frac{1}{\bar{N}}\int_{T'}^{T''} \bar{g}_1(T)\mathrm{e}^{-\beta T}\,dT\left(2 - \int_{T'}^{T''} p_T(T)\mathrm{e}^{\beta T}\,dT\right), \tag{15}$$

so, taking into account Eq. (10), we obtain

$$f_1 = 2 - \int_{T'}^{T''} p_T(T)\mathrm{e}^{\beta T}\,dT\,. \tag{16}$$

The fractions in S and G2M, f_S and f_{G2M}, can be written by integrating the density $\nu(a,T)$ between suitable limits. In Appendix A we report these fractions together with approximated expressions in terms of mean values and standard deviations of phase transit times. The above equations can easily be extended to the case in which the rate constants of cell loss from the two compartments are different (Bertuzzi and Gandolfi, 1999).

We stress that the theory of this section does not provide a dynamic model for the evolution of the cell population, because the rate of exit from compartment 1 is not prescribed and thus the asymptotic growth rate α cannot be calculated. The above equations allow to describe, within a time horizon not too large (as it will be specified in the next subsection), the age structure in AEG of those cell subpopulations that determine the evolution of the quantities measured in a labelling experiment.

3.2. Labelled subpopulations after pulse labelling

Because some experimental evidences suggest that the BrdUrd concentration decays rapidly after the injection into the tumour-bearing animal, the labelling process is often considered as truly impulsive. In other words, if label is injected at time $t=0$, it is assumed that at $t=0^+$ all cells in S phase are labelled. Under this assumption, the time course of the fraction of labelled cells can be easily computed from model equations. Because the labelled cells begin to divide at times larger than the minimum duration of G2M phase, a subpopulation of labelled divided cells arises after that time. Thus, a fraction of labelled undivided cells and a fraction of labelled divided cells can be distinguished (see Fig. 1). The time course of the mean DNA content of the labelled undivided cells can also be computed. This quantity is measured by the "relative movement" (Begg *et al.*, 1985), that is the difference of the mean PI fluorescence of the labelled undivided cells and the mean PI fluorescence of G1 cells, normalized to the increment of fluorescence from G1 to G2M cells.

Let us consider initially a cell population obeying assumptions (i)-(iv) of section 3.1, $T = T_S+T_{G2M}$ being constant over the population. It is easy to see that the fractional cell density with respect to age in S+G2M has the expression

$$\nu_T(a) = \beta \mathrm{e}^{\beta T} \mathrm{e}^{-\beta a}\,, \quad a \in [0,T]\,, \tag{17}$$

having indicated by a subscript the dependence on T. In this case, the time course of the fraction of labelled undivided cells, f_T^{lu}, and of the fraction of labelled divided cells, f_T^{ld}, are given by (White *et al.*, 1990)

$$f_T^{lu}(t) = \begin{cases} \mathrm{e}^{\beta(T-t)} - \mathrm{e}^{\beta(T_{G2M}-t)} & 0 \le t \le T_{G2M} \\ \mathrm{e}^{\beta(T-t)} - 1 & T_{G2M} \le t \le T\,. \end{cases} \tag{18}$$

$$f_T^{ld}(t) = \begin{cases} 0 & 0 \le t \le T_{G2M} \\ 2[1 - \mathrm{e}^{-\beta(t-T_{G2M})}] & T_{G2M} \le t \le T \\ 2[\mathrm{e}^{-\beta(t-T)} - \mathrm{e}^{-\beta(t-T_{G2M})}] & T \le t \le T_{G2M}+T_{1min}+T\,. \end{cases} \tag{19}$$

Denoting by $x(a,T)$ the DNA content of a cell of age a, the mean DNA content of the labelled undivided cells at time t, $\langle x \rangle_T^{lu}(t)$, is given by

$$\langle x \rangle_T^{lu}(t) = \frac{\displaystyle\int_t^{\min[T_S+t,T]} x(a,T)\nu_T(a)\,da}{\displaystyle\int_t^{\min[T_S+t,T]} \nu_T(a)\,da}\,, \tag{20}$$

with $x(a,T)$ obtained as

$$x(a,T) = \begin{cases} 1 + \int_0^a v(s,T)\,ds\,, & 0 \le a \le T_S \\ 2 & T_S < a \le T\,, \end{cases} \tag{21}$$

where $v(a,T)$ is the rate of DNA synthesis (DNA amount synthesized in the unit time) of a cell of age a. Assuming the DNA content x of G1 cells equal to 1 and the mean PI fluorescence of a cell proportional to the DNA content of that cell, the relative movement of the labelled undivided cells can be expressed as

$$RM_T(t) = \langle x \rangle_T^{lu}(t) - 1\,. \tag{22}$$

If the rate of DNA synthesis is constant across S phase, the relative movement is given by (White and Meistrich, 1986)

$$RM_T(t)=\begin{cases}\dfrac{1+\beta t-\mathrm{e}^{-\beta(T_S-t)}-\beta T_S\mathrm{e}^{-\beta T_S}}{\beta T_S(1-\mathrm{e}^{-\beta T_S})} & 0\le t\le T_{G2M}\\ \dfrac{1+\beta t-\mathrm{e}^{-\beta(T_S-t)}-\beta T_S\mathrm{e}^{-\beta(T-t)}}{\beta T_S(1-\mathrm{e}^{-\beta(T-t)})} & T_{G2M}\le t\le T_S.\end{cases} \tag{23}$$

An expression of the relative movement for a class of nonconstant rates of DNA synthesis was proposed by Bertuzzi et al. (1995a).

Let us now consider the case of distributed T: we have from Eq. (13) that

$$\nu(a,T)=p_T(T)\nu_T(a)\,. \tag{24}$$

We notice that a definition for the frequency function of T different from that given in Eq. (8), for instance referring to cells entering S phase, would lead to a relation between ν and ν_T not so simple as (24) and involving the parameter β. For the fraction of labelled undivided cells, $f^{lu}(t)$, we thus obtain

$$\begin{aligned}f^{lu}(t)&=\int_{T'}^{T''}\int_t^{\min[T_S(T)+t,T]}\nu(a,T)\,da\,dT=\int_{T'}^{T''}p_T(T)\int_t^{\min[T_S(T)+t,T]}\nu_T(a)\,da\,dT\\&=\int_{T'}^{T''}p_T(T)f_T^{lu}(t)\,dT\,,\end{aligned} \tag{25}$$

with f_T^{lu} given by (18), where T_{G2M} has now to be read as $T_{G2M}(T)$. Let us define the time $t^\star=T_{G2M}(T')+T_{1min}$. For $t<t^\star$ the labelled divided cells are confined in compartment 1, so that, taking into account (12), we have for the fraction of labelled divided cells, $f^{ld}(t)$, the following expression

$$f^{ld}(t)=\int_{T'}^{T''}\int_{\max[0,t-T]}^{\max[0,t-T_{G2M}(T)]}\nu_1(a_1,T)\,da_1dT=\int_{T'}^{T''}p_T(T)f_T^{ld}(t)\,dT\,. \tag{26}$$

We observe that a strict relationship exists between $f^{lu}(t)$ and $f^{ld}(t)$. For times preceding the second round of division of the labelled cells, it is in fact

$$N^{lu}(t)+\frac{1}{2}N^{ld}(t)=N_S(0)\mathrm{e}^{-\beta t} \tag{27}$$

where N^{lu} and N^{ld} are the number of labelled undivided and, respectively, labelled divided cells and N_S is the number of cells in S phase. Dividing by $N(t)$, in AEG we obtain the equation

$$f^{lu}(t)+\frac{1}{2}f^{ld}(t)=f_S\mathrm{e}^{-\beta t}\,, \tag{28}$$

that provides a rapid way to estimate β and to obtain a first approximation of $\langle T_S\rangle$ (see *A*.3).

The mean DNA content of the labelled undivided cells is given by

$$\langle x\rangle^{lu}(t)=\frac{\displaystyle\int_{T'}^{T''}\int_t^{\min[T_S(T)+t,T]}x(a,T)\nu(a,T)\,da\,dT}{\displaystyle\int_{T'}^{T''}\int_t^{\min[T_S(T)+t,T]}\nu(a,T)\,da\,dT}\,, \tag{29}$$

where $x(a,T)$ now denotes the DNA content of a cell of class T and age a. From (24), (29) and (22) we get for the relative movement $RM(t)$

$$RM(t) = \frac{\int_{T'}^{T''} p_T(T) RM_T(t) f_T^{lu}(t)\, dT}{\int_{T'}^{T''} p_T(T) f_T^{lu}(t)\, dT}\,, \tag{30}$$

where T_S in the expressions (20) and (21) has to be read as $T_S(T)$.

The derivation of explicit expressions for the above quantities is rather cumbersome. As an example, we give in Appendix B the expressions for the fraction of labelled undivided cells assuming $T_S(T)=\gamma T$, $\gamma \in (0,1)$.

3.3. Non-impulsive labelling

Some experimental evidences *in vitro* (Powell *et al.*, 1990; Starace and Santoro, unpublished results) show that very low BrdUrd concentrations produce detectable labelling. After the BrdUrd injection in the animal, the label concentration in the fluids surrounding the tumour cells changes with the time and eventually vanishes. Thus, for a more general description of the *in vivo* labelling process, we have considered a continuous labelling in conditions of variable label concentration (Bertuzzi and Gandolfi, 1997; Bertuzzi and Gandolfi, 1999). Because a cell with age a in S+G2M at time t after the BrdUrd injection has entered S phase at time $t-a$, we can write for the amount $b(a,t,T)$ of BrdUrd that has been incorporated up to time t in the DNA of a cell of class T having age a the following equation:

$$b(a,t,T) = \int_{t-a}^{t} \zeta(s+a-t,s,T)\, ds\,, \tag{31}$$

where $\zeta(a,t,T)$ is the rate at which BrdUrd is incorporated into a cell of class T with age a at time t. Since the BrdUrd molecules rapidly traverse the cell membrane, we write ζ as a function of the extracellular BrdUrd concentration $c(t)$ and of the DNA synthesis rate $v(a,T)$ (v being nonzero for $0 \le a \le T_S(T)$). The amount of incorporated BrdUrd has shown a saturable behaviour with respect to the extracellular BrdUrd concentration in cell cultures (Kriss and Revesz, 1961). Because the initial value of the BrdUrd concentration in mice could exceed the saturating concentration, we assume for ζ the following expression

$$\zeta(a,t,T) = q\, v(a,T) \frac{c(t)}{\bar{c} + c(t)} \tag{32}$$

where q and $\bar{c}$ are constants depending on cellular parameters.

For times larger than the minimum duration of G2M phase, the amount b_1 of BrdUrd present into a cell of compartment 1, that has been generated by a cell of class T and has age a_1 at time t, is given by

$$b_1(a_1,t,T) = \frac{1}{2}\, b(T, t-a_1, T)\,. \tag{33}$$

Note that $b_1 = 0$ if $t - a_1 < T_{G2M}(T)$.

If cells are considered to be labelled when they contain a whatever small amount of label, in the case of $c(t) > 0$ for $0 < t < t^\star$, the fractions of labelled undivided and divided cells at time t are given by

$$f^{lu}(t) = \int_{T'}^{T''} \int_{0}^{\min[T_S(T)+t,T]} \nu(a,T)\, da dT \tag{34}$$

$$f^{ld}(t) = \int_{T'}^{T''} \int_{0}^{\max[0,t-T_{G2M}(T)]} \nu_1(a_1, T)\, da_1 dT \tag{35}$$

for $0 \leq t \leq t^\star$.

These expressions, however, do not take into account that the cells are identified as labelled if the intensity of the green fluorescence exceeds a threshold value. Thus, minute amounts of BrdUrd, that are possibly incorporated in conditions of decreasing label concentration, can be unable to label effectively the cells. To obtain a correct expression of the measured fractions of labelled undivided and divided cells, is therefore convenient to write the DNA-BrdUrd fluorescence distribution obtained by flow cytometry.

3.4. DNA-BrdUrd fluorescence distribution and observable quantities

To find an expression for the DNA-BrdUrd distribution, let us denote by y and z the intensities of red (PI) and, respectively, green (FITC) fluorescence of a cell measured by the flow cytometer. The quantity y depends on the amount of fluorochrome bound to DNA, and then on the DNA content of the cell, whereas z is related to the amount of BrdUrd incorporated into the cell. Because of the instrumental and staining sources of variability, the measured y and z of cells with the same DNA content x and BrdUrd content b will be different, and it appears thus reasonable to consider y and z as independent random variables. Fluorescence dispersion can be represented by defining a conditional probability density function (pdf) $P_y(y|x)$ for the red fluorescence intensity y of a cell with DNA content x ($x \in [1, 2]$), and a conditional pdf $P_z(z|b, x)$ for the green fluorescence z of a cell with BrdUrd content b and DNA content x. As commonly accepted (Bagwell, 1993), $P_y(y|x)$ has been assumed as a gaussian distribution with mean $m(x)$ and standard deviation (SD) $\sigma_y(x)$. The fluorescence mean is approximately proportional to x and a more accurate representation is $m(x) = y_1 + (y_2 - y_1)(x - 1)$, y_1 and y_2 being the mean red fluorescences of G1 and G2M cells, respectively. Since the SD of PI fluorescence increases with the DNA content and the coefficient of variation is possibly not constant, we assumed $\sigma_y(x) = \sigma_1 x^r$, with $r \geq 0$, where σ_1 is the SD of the fluorescence of cells with $x = 1$. Similarly, the pdf $P_z(z|b, x)$ can be defined as a gaussian distribution, where the mean value of z is the sum of a contribution hb due to incorporated BrdUrd (h being a constant depending on the experimental procedure), and of an aspecific contribution $d(x)$ due to cell autofluorescence. Autofluorescence appears to increase with cell mass, and so with the position of the cell in the cycle; thus we assumed $d(x) = z_1 + (z_2 - z_1)(x - 1)$, where z_1 and z_2 are the mean green fluorescences of unlabelled cells in G1 and G2M, respectively. For the SD of green fluorescence, $\sigma_z(b, x)$, we simply took a constant coefficient of variation CV_z, so $\sigma_z(b, x) = CV_z(hb + d(x))$.

Denoting by $\rho(y, z, t)$ the joint pdf of y and z at time t, we have

$$\rho(y, z, t) = \rho_1^u(y, z, t) + \rho_1^l(y, z, t) + \rho_2(y, z, t) \tag{36}$$

where ρ_1^u and ρ_1^l are the contributions of unlabelled ($b_1 = 0$) and, respectively, labelled ($b_1 > 0$) cells in compartment 1, and ρ_2 is the contribution of cells in compartment 2, both labelled ($b > 0$) and unlabelled ($b = 0$). Thus, for $0 \leq t \leq t^\star$, we can write the following equations:

$$\rho_1^u(y, z, t) = P_y(y|1) P_z(z|0, 1)(f_1 - f^{ld}(t)) \tag{37}$$

$$\rho_1^l(y, z, t) = P_y(y|1) \int_{T'}^{T''} \int_{0}^{\max[0,t-T_{G2M}(T)]} P_z(z|b_1(a_1, t, T), 1) \nu_1(a_1, T)\, da_1 dT \tag{38}$$

$$\rho_2(y,z,t) = \int_{T'}^{T''} \int_0^T P_y(y|x(a,T)) P_z(z|b(a,t,T),x(a,T)) \nu(a,T)\, da dT \tag{39}$$

where f_1 and $f^{ld}(t)$ are given by Eqs. (16) and (35), $b(a,t,T)$ and $b_1(a,t,T)$ are given by Eqs. (31)-(32) and (33). We note that the distribution of the green fluorescence z for a given value of y depends, in the present model, both on the instrumental and staining sources of variability and on the presence of cells that have different BrdUrd content because of the different rates of progression across S phase.

In principle, $\rho(y,z,t)$ might be directly compared with the experimental bivariate DNA-BrdUrd histograms. However, this is not convenient due to the low statistical representativeness of the experimental points in a two-dimensional plot. Thus the comparison has been attempted at an intermediate level using monoparametric distributions derived from ρ together with appropriately selected integrals. In the experimental setting, a DNA-BrdUrd histogram can be elaborated at different levels. Initially, the cells are identified as labelled (or BrdUrd+) if the intensity of green fluorescence exceeds a threshold value fixed by the experimenter according to the level of cell autofluorescence. The labelled cells are additionally subdivided into labelled undivided and labelled divided (on the basis of a gap in the red fluorescence distribution of labelled cells), and the fractions of these cells are actually measured. In this work we went further in the data analysis, obtaining the distribution of the BrdUrd+ cells with respect to y and the mean green fluorescence of the BrdUrd+ cells as a function of y. Comparison of the experimental results and model could be performed at this level, since the time evolution of these functions can be theoretically derived from $\rho(y,z,t)$ as follows. Let $\bar{z}$ be the threshold value of green fluorescence and $\bar{y}$ be the threshold value of red fluorescence that separates the undivided from the divided cells. The fractional density with respect to y of the positive cells $p^+(y,t)$, can be computed as

$$p^+(y,t) = \int_{\bar{z}}^{\infty} \rho(y,z,t)\, dz\,, \tag{40}$$

and the mean green fluorescence as a function of y of the positive cells, $\langle z\rangle^+(y,t)$, as

$$\langle z\rangle^+(y,t) = \frac{\int_{\bar{z}}^{\infty} z\rho(y,z,t)\, dz}{p^+(y,t)}\,. \tag{41}$$

Based on the theoretical distribution $\rho(y,z,t)$, it is now possible to give expressions for f^{lu}, RM, and f^{ld} that, compared to equations (25), (26) and (30), should more closely represent the measured quantities. We have

$$f^{lu}(t) = \int_{\bar{y}}^{y''} p^+(y,t)\, dy\,, \tag{42}$$

$$RM(t) = \frac{1}{y_2 - y_1}\left(\frac{\int_{\bar{y}}^{y''} y\, p^+(y,t)\, dy}{\int_{\bar{y}}^{y''} p^+(y,t)\, dy} - y_1\right), \tag{43}$$

$$f^{ld}(t) = \int_{y'}^{\bar{y}} p^+(y,t)\, dy\,, \tag{44}$$

where $y' < y_1$ and $y'' > y_2$ are reasonable lower and upper limits for the red fluorescence intensity of tumour viable cells. When labelled divided cells are not present, $\bar{y}$ is set to y' in the above formulas.

Since various steps (denaturation, antibody reactions, etc.) in the preparation of cells for DNA-BrdUrd flow cytometry introduce a large variability from sample to sample in the level of green fluorescence, the mean green fluorescence profile of Eq. (41) was normalized to the following mean fluorescence:

$$\langle \tilde{z} \rangle(t) = \frac{\int_{y'}^{y''} \int_{\bar{z}}^{\infty} z\rho(y,z,t)\, dz\, dy}{f^{lu}(t) + 0.5\, f^{ld}(t)} \,. \tag{45}$$

It can be seen that, in the case of impulsive labelling, the mean fluorescence in (45) is approximately proportional to the mean BrdUrd content of a labelled cell immediately after labelling and thus, in principle, it should provide a reference value constant with the time. In fact, after compensating for cell loss, the total amount of BrdUrd in the cell population (proportional to the numerator of (45)) remains constant and the same holds for the sum of the labelled undivided cells plus half the labelled divided cells (proportional to the denominator of (45)).

3.5. Model parameters

The theoretical time-course of the observable quantities depends on the parameters and functions that characterize both the kinetics of the tumour cell population and the process of labelling and measurement. We have chosen to represent the distribution $p_T(T)$ as uniform between T' and T''. Numerical simulations have indeed shown that the observables depend only to a little extent on the moments of order higher than the second (Bertuzzi and Gandolfi, 1999). For the function $T_S(T)$, we have chosen for simplicity $T_S(T) = \gamma T$, $\gamma \in (0,1)$, so the durations of S and G2M phases are uniformly affected by the lengthening of T. Moreover, the rate of DNA synthesis was assumed as a downward concave parabolic function with respect to the DNA content x, $w(x,T)$, having the maximum at $\bar{x} \in (1,2)$ and the value at $x=1$ equal to a fraction k of the maximum, whose value will depend on $T_S(T)$. From $w(x,T)$, as shown in Appendix C, the function $v(a,T)$ is computed by means of a variable transformation.

Assuming pulse labelling, the fractions of labelled cells and the relative movement as given by the equations (25), (26) and (30), will thus depend on the following tumour kinetic parameters: β (or, equivalently, T_{pot} as usual in the biological literature), T', T'', γ, $\bar{x}$, and k.

To obtain the observable quantites by means of equations (40)-(45), the following measurement parameters have to be specified: y_1, y_2, $\bar{y}$, z_1, z_2, $\bar{z}$, σ_1, r, CV_z, and the product hq. The thresholds $\bar{z}$ and $\bar{y}$ are fixed by the experimenter, whereas y_1, y_2, z_1, z_2, σ_1, r, and CV_z can be estimated from the bivariate histograms using the software currently available with the flow cytometer. For this purpose, a histogram measured immediately after the BrdUrd administration is particularly useful, because the subpopulations of unlabelled cells with DNA content equal to 1 and 2 can be easily recognized. In the following we have rescaled y to have $y_1 = 1$ and $y_2 = 2$. The product hq appears to be highly variable among histograms and cannot be accurately estimated *a priori*. An approximate value has been obtained with reference to the histograms at $t = 0.5$ h, in which the maximal value of the mean green fluorescence $\langle z \rangle^+$ is around 2×10^3, assuming the mean rate of DNA synthesis of 0.04 h^{-1} and the effective duration of the labelling of 0.5 h. Thus $hq = 10^5$ was obtained and this value was used in all the simulations. However, when hb is much larger than the threshold $\bar{z}$, the influence of hq on the computation of the fraction of positive cells is reduced. Moreover, hq appears as a multiplicative factor of the mean green fluorescence and thus the intersample staining variability can be neglected if $\langle z \rangle^+(y,t)$ is considered after suitable normalization.

To take into account the non-impulsive labelling, we have chosen to represent the BrdUrd concentration $c(t)$ by a decreasing exponential function with time constant τ, that is $c(t) = c_0 e^{-t/\tau}$. So two additional parameters are introduced, τ and the ratio $\bar{c}/c_0$. Whereas τ is actually unknown, a value to the ratio $\bar{c}/c_0$ can be assigned by assuming $\bar{c} = 4\,\mu$M, as deduced from the data of Kriss and Revesz (1961), and computing c_0 as the ratio of the BrdUrd dose to the distribution volume of the animal (estimated as 20 ml in mice).

4. Results

Experimental data were preliminarly analyzed according to the method proposed by White *et al.* (1990), that is by simultaneous fitting of f^{lu}, f^{ld} and RM data by means of Eqs. (18), (19) and (23), respectively. This method assumes no cell-to-cell variability of phase transit times, constant rate of DNA synthesis across S phase and pulse labelling, and allows the estimation of T_S, T_{G2M} and T_{pot} ($T_{pot} = \log 2/\beta$). These parameters, obtained by minimizing the sum of squared deviations for f^{lu}, f^{ld} and RM, are reported in Table 1 (row A) together with the value of the residual sum of squares (RSS). The estimates, that predicted an exceedingly short duration of the G2M phase, gave a poor fitting of the data, particularly for RM and f^{ld} (see the RM in Fig. 3).

Table 1. Estimates of tumour kinetic parameters. A, B, C, and D refer to different models, as explained in the text.

	T_{pot} (h)	T_S (h)	T_{G2M} (h)	RSS
A	136.48	32.86	2.80	0.1033
B	122.09	28.47	4.89	0.0341
C	112.37	25.88 (7.00)[a]	5.18 (1.40)[a]	0.0292
D	110.41	23.49 (8.36)[a]	5.25 (1.87)[a]	0.0277

[a] Mean value (SD) of the quantity over the cell population

A first, marked improvement of the fitting was achieved by introducing a nonconstant rate of DNA synthesis across S phase. The profile of the incorporated BrdUrd across S phase, and then the profile of the mean green fluorescence at a short time after the label injection, closely reflect the pattern of the rate of DNA synthesis, as can be seen from Eqs. (30)-(31) (see also Bertuzzi *et al.*, 1995b). To obtain an estimate of the profile of the rate of DNA synthesis, we determined the parameters $\bar{x}$ and k of the expression ($C.1$)-($C.2$) in appendix C by least squares fitting of $C.1$ (suitably normalized) to the data of the normalized mean green fluorescence at 0.5 h. We found $\bar{x} = 1.630$ and $k = 0.221$, that provided a satisfactory fitting. By using Eqs. (18), (19) and (20)-(22), with the expression ($C.4$) for $x(a)$, to fit the data, we obtained the kinetic parameters reported in Table 1 (row B). The value of the residual sum of squares decreased from 0.1033 to 0.0341 and the time course of the RM is shown in Fig. 3. However, in spite of the improvement obtained, the predicted RM fails to show the downward curvature suggested by the data at the late time points.

Assuming now the presence of heterogeneity of transit time in S and G2M, as described by the model of Section 3, we used the expressions (25), (26) and (30) to fit the experimental data. The least squares estimation gave the following estimates: $T_{pot} = 112.37$ h, $T' = 16.50$ h, $T'' = 45.60$ h (so we have $\langle T \rangle = 31.05$ h for the mean value of T, and for the standard deviation $\mathrm{SD}(T) = 8.40$

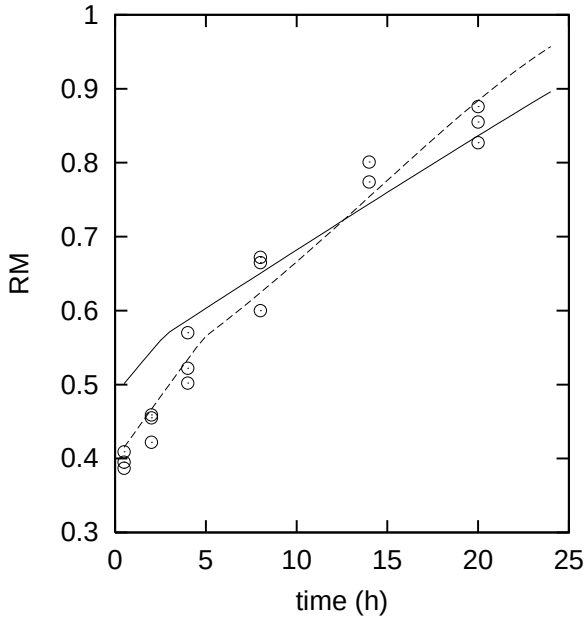

Fig. 3. Experimental data of the relative movement together with the theoretical curves obtained by the model with constant DNA synthesis rate (continuous line, parameters in Table 1 row A), and by the model with parabolic DNA synthesis rate (dashed line, parameters in Table 1 row B).

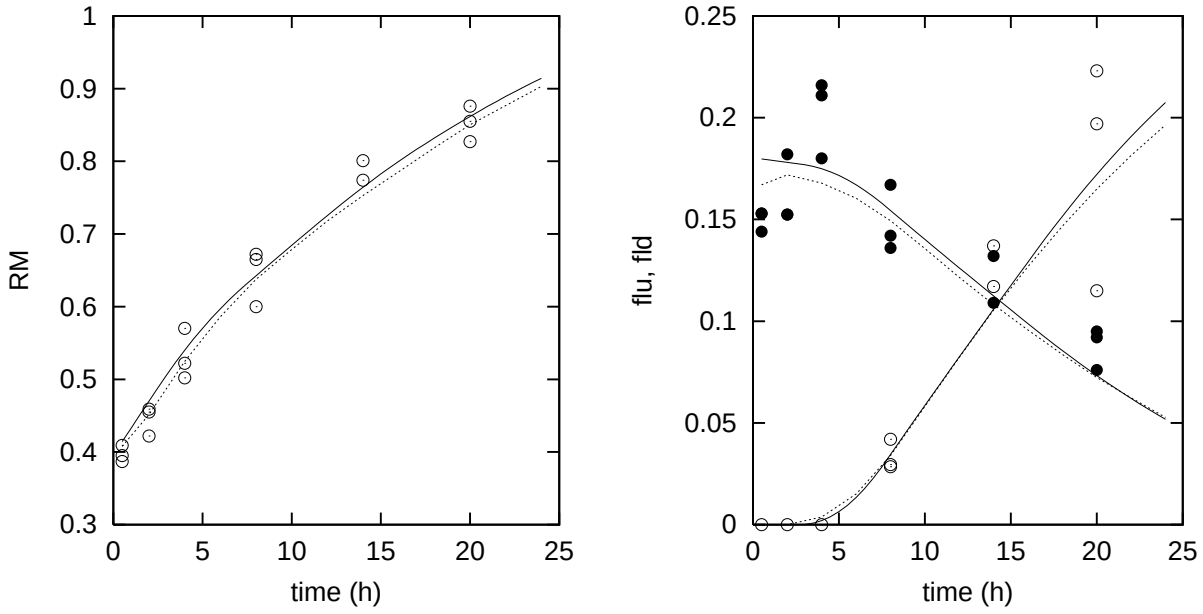

Fig. 4. Left panel: experimental data of the relative movement. Right panel: experimental data of the fractions of labelled undivided (closed symbols) and labelled divided (open symbols) cells. Both panels: optimal fitting curves obtained by the model with kinetic heterogeneity and pulse labelling (continuous line, parameters in Table 1 row C), and by the model with kinetic heterogeneity and nonimpulsive labelling (dotted line, parameters in Table 1 row D).

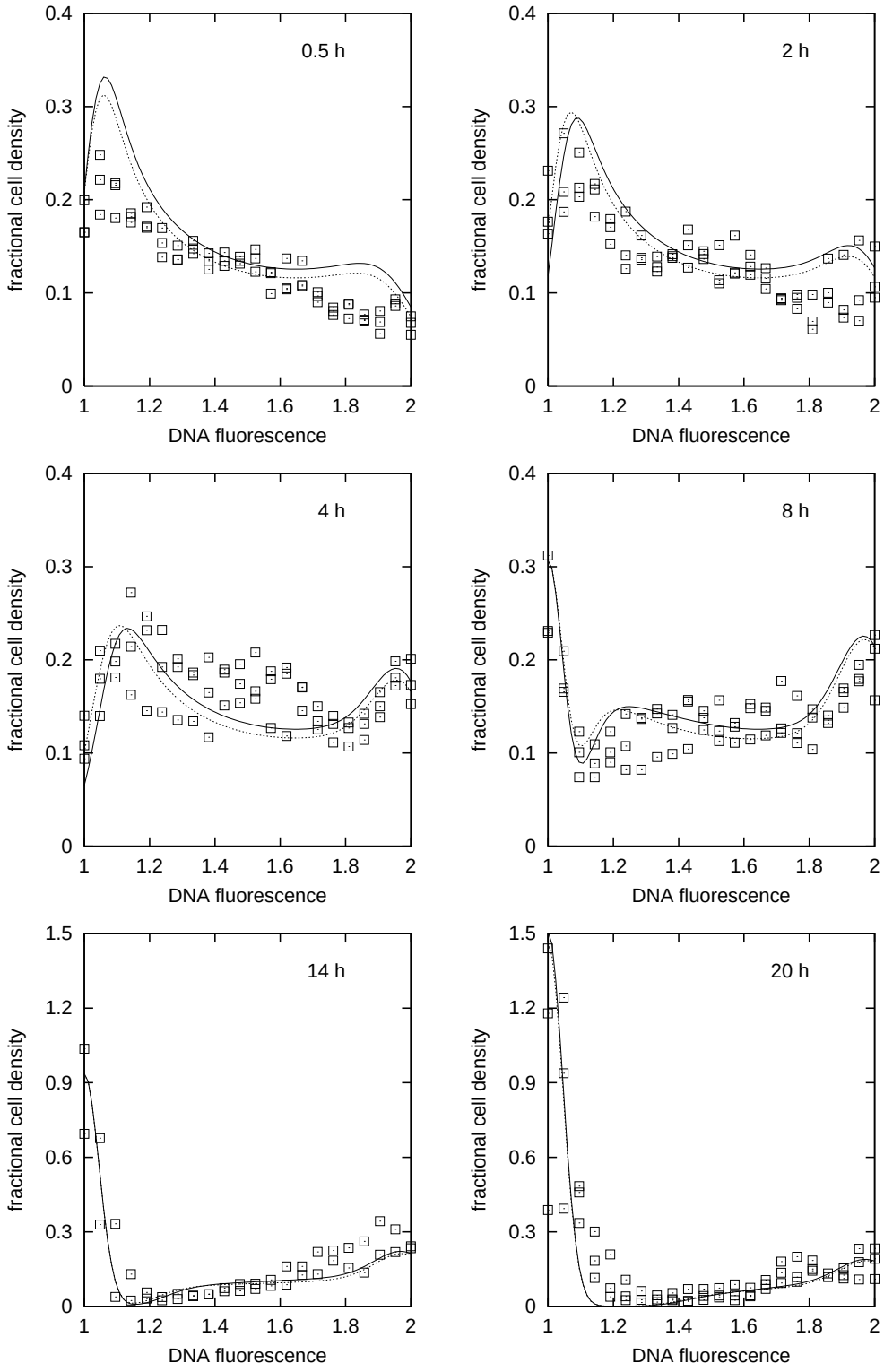

Fig. 5. Experimental data of the fractional density of positive cells with respect to the red fluorescence. Predictions obtained by the model with kinetic heterogeneity and pulse labelling (continuous line, parameters in Table 1 row C), and fitted profiles obtained by the model with kinetic heterogeneity and nonimpulsive labelling (dotted line, parameters in Table 1 row D).

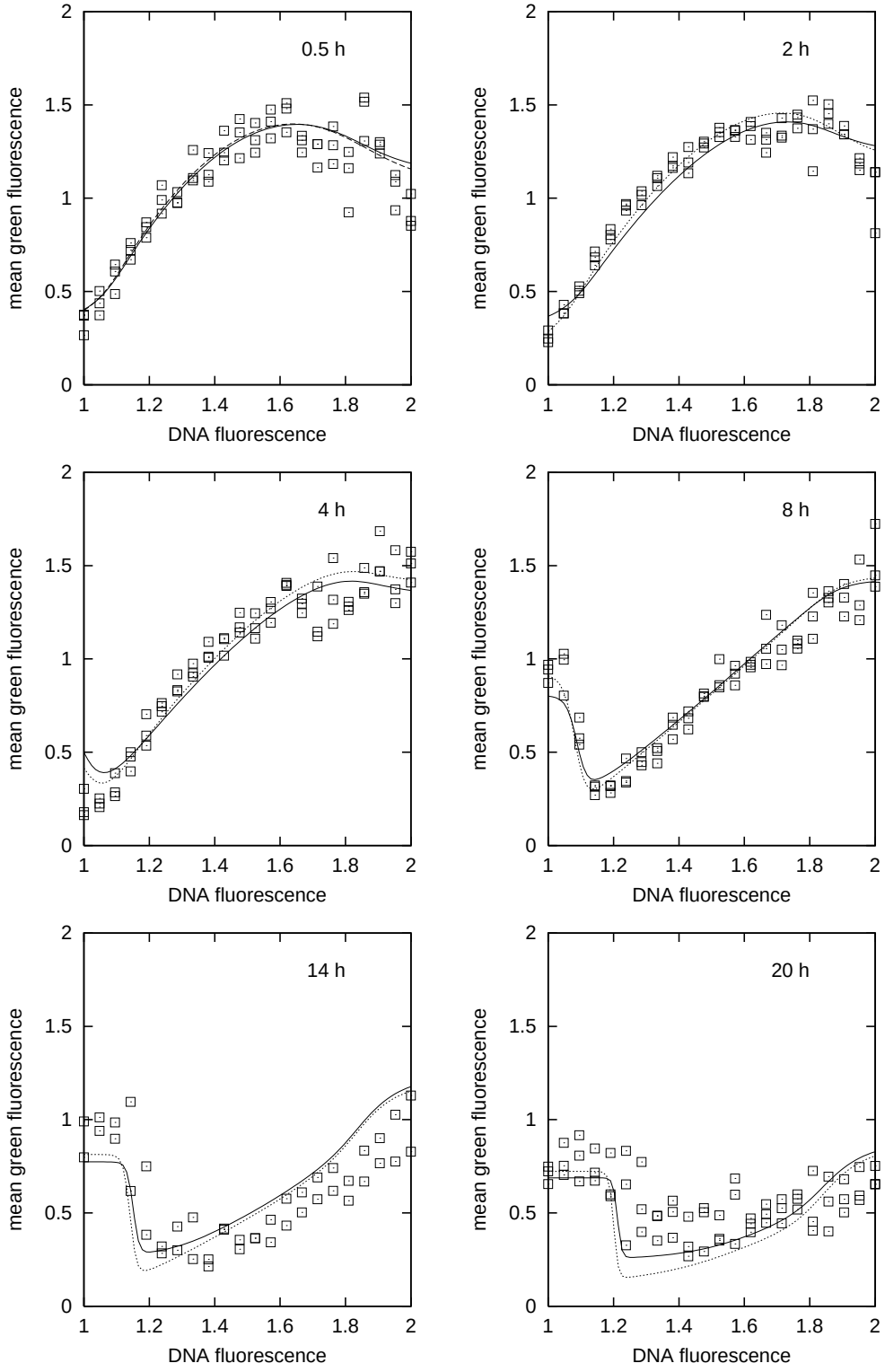

Fig. 6. Experimental data of the mean green fluorescence of positive cells with respect to the red fluorescence. Predictions obtained by the model with kinetic heterogeneity and pulse labelling (continuous line, parameters in Table 1 row C), and fitted profiles obtained by the model with kinetic heterogeneity and nonimpulsive labelling (dotted line, parameters in Table 1 row D).

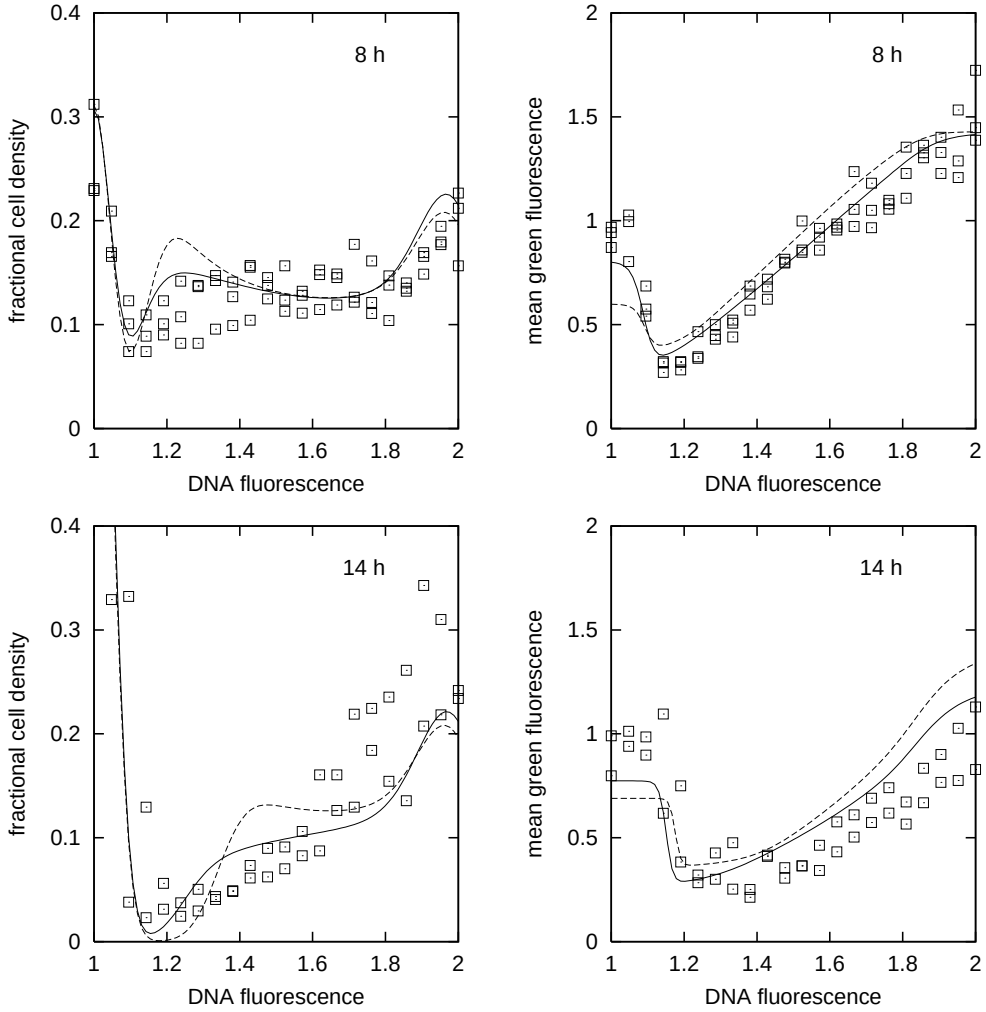

Fig. 7. Comparison of the profiles of the fractional density and of the mean green fluorescence of the positive cells with respect to the red fluorescence obtained by the model with kinetic heterogeneity and pulse labelling (continuous line, parameters in Table 1 row C), and by the model without kinetic heterogeneity (dashed line, parameters in Table 1 row B).

h), and $\gamma = 0.833$. The corresponding mean and SD values of T_S and T_{G2M} are reported in Table 1 (row C) and the time courses of f^{lu}, RM and f^{ld} are reported in Fig. 4. The heterogeneity in T_S and T_{G2M} allowed a better fitting, as shown by the reduction in the RSS value and by the curvature presented by the relative movement that more accurately follows the profile of the data. It is observed, however, that the f^{lu} data suggest an initial increase of the labelled fraction, that it is not possible to achieve by any model assuming impulsive labelling. Using the previous estimates of the kinetic parameters (Table 1 row C), according to the theory of section 3.4, the time course of the profiles of the fractional density with respect to the red fluorescence of positive cells and the normalized profile of the mean green fluorescence of positive cells can be predicted through Eqs. (40) and (41),(45). Figures 5 and 6 show these predictions. The measurement parameters were fixed at the following values: $z_1 = 10$, $z_2 = 20$, $\sigma_1 = 0.045$, $r = 1$, $CV_z = 0.2$, $hq = 10^5$. Overall, the prediction of the profiles appears satisfactory and they give further evidence of the presence of kinetic heterogeneity. The fractional density and the mean green fluorescence predicted by the model without heterogeneity (parameters in row B of Table

1) give indeed a worse agreement with the data at the late times (see a comparison in Fig. 7). The adequacy of the assumed pattern of the rate of DNA synthesis is confirmed by the good prediction of the mean green fluorescence data at 0.5 h.

From the estimate of T_{pot} and from the doubling time of the tumour, $T_d = 9.8$ days, the cell loss factor, defined as $1 - T_{pot}/T_d$ (Steel, 1977), can be computed yielding 0.52, a rather high value.

To evaluate the effect of a nonimpulsive labelling on the prediction of the data, we selected by a trial-and-error procedure a value of the pharmacokinetic time constant τ and values of the tumour kinetic parameters that further improve the RSS of the fitting of RM, f^{lu} and f^{ld} data. These values are: $\tau = 0.206$ h^{-1}, $T_{pot} = 110.41$ h, $T' = 11.02$ h, $T'' = 46.45$ h (so $\langle T \rangle = 28.74$ h and SD$(T) = 10.23$ h), and $\gamma = 0.817$. We note that with $\tau = 0.206$ h^{-1}, according to Eq. (32) and to the assumed values for c_0 and $\bar{c}$, the rate of BrdUrd incorporation halves its value after 0.85 h from the label injection. The mean and SD values of T_S and T_{G2M} are reported in Table 1 (row D), showing a slightly faster kinetics of the cell population, and the time courses of RM, f^{lu} and f^{ld} are reported in Fig. 4. An initial increase in the theoretical time course of f^{lu} is now seen to be present. The prediction of the fractional densities and the normalized mean green fluorescences are shown in Figs. 5 and 6. Concerning the RSS of these curves there is an overall slight improvement with respect to the estimate C, except for the data of mean green fluorescence at 20 h. However, for the data in Fig. 6 at 20 h in the early S phase, we notice that the experimental values of mean green fluorescence in the region of red fluorescence between 1.2 and 1.4 refer to a small number of events (around 10-20), so that contaminants such as aggregates or dead cells may mask the actual viable cells.

Since a rigorous estimation procedure involving all the data would require an accurate analysis of their statistics, which is beyond the scope of the present paper, the curves obtained by the parameter values of row D in Table 1 are only indicative of the possible response of the model. However, it is seen that the assumption of nonimpulsive labelling in the case of *in vivo* experiments appears to be necessary to account for particular features of f^{lu} data.

5. Conclusions

The study of the *in vivo* cell proliferation is a key issue in cancer research, representing the level where the cellular description of the pathology and the strategy of therapy converge. The precise knowledge of the cell kinetics of experimental tumours allow a deeper evaluation of the effects of antiproliferative treatments. The introduction of BrdUrd techniques represented a very important step in the attempt of reaching a quantitative description of the behaviour of cell populations in that they made some kinetics features measurable, as in the case of the T_{pot}, even in the clinical setting. Nevertheless, the major usage of BrdUrd is still aimed only at deriving, using simple formulae, two synthetic descriptors of kinetics, like T_S and T_{pot}, for prognostic purposes, somewhat overlooking the wider amount of information contained in flow cytometric data, bearing on the kinetic heterogeneity of the tumour.

This work is aimed to a thorough retrieval of the information contained in the time course of the BrdUrd flow cytometric data obtained in an *in vivo* experimental setting. This is performed by connecting the observable data with a not elementary mathematical model of cell proliferation that includes the description of the cell cycle phases with inter-cell variability of transit times, a nonconstant rate of DNA synthesis, and the pharmacokinetics of BrdUrd. We found that, at this level of complexity, a more satisfactory and comprehensive explanation of the data can

be obtained, conversely meaning that information on these features might be retrieved from BrdUrd data.

However, we are aware that technical problems impair a direct attempt to retrieve a precise measure of the variability of phase transit times in the tumour. They arise both in sample preparation and in flow cytometric data processing. The experimental tumour model adopted in the present work, a human ovarian cancer line (HOC18) growing in nude mice, is not free from these technical difficulties, although representing a favourable case. First, the HOC18 cell population is aneuploid, allowing to distinguish and rule out the G1 normal diploid cells, which always are present in tumour cell preparations. The S and G2M normal diploid cells are counted within the region of tumour cells in the flow cytometric dot plot, but this contaminant is negligible (<1%) in our case. Second, during sample preparation aggregates may be produced, causing two G1 cells to be detected as a G2 cell. Electronic gating is compulsory to rule out these artefacts. However, imperfect recognition of aggregates may contribute to the low sensitivity of our data to the outgoing of G2M BrdUrd− cells and may contaminate the subpopulations relevant to the analysis. Third, the positioning of the levels that discriminate BrdUrd negative from positive or divided from undivided cells may convey an element of uncertainty. In our case, little doubt exists in distinguishing divided from undivided cells, due to the long G1 phase of HOC18 cells. However, the setting of the threshold separating BrdUrd negative from positive cells was somewhat arbitrary, and the amount of uncertainty in the percentage of BrdUrd+ cells, evaluated as less than 2%, may contribute to some discrepancy between the fitting and the experimental profile of BrdUrd+ cells near G1. Thus, with our experimental model we could reasonably overcome a series of methodological problems and use a time sequence of data to reveal some of the underlying biological heterogeneity. On the other hand, the use of different animals for each data point introduces a further source of variability. The experimental design focused on BrdUrd positive cells, also considering the profile of mean green (BrdUrd) fluorescence at different time points. The adopted internal normalization for these profiles yielded data unaffected by inter-sample staining variability.

The application of the proposed mathematical model, representing the tumour cell population and the measurement process, to our data has evidenced a substantial degree of heterogeneity in the transit times through S and G2M phases. This confirms previous findings by Baisch and Otto (1993) and Baisch *et al.* (1995), giving further evidence to this feature of the *in vivo* tumour cell kinetics. The presence of heterogeneity, quantitated by the analysis of the relative movement together with the fractions of labelled undivided and labelled divided cells, was confirmed by the time evolution of the fractional density and the mean green fluorescence of labelled cells. The variability of the rate of DNA synthesis across S phase was found to be a crucial feature for the kinetic analysis. To this end, the use of the mean green fluorescence as a function of the red fluorescence represented an essential step in assessing the pattern of this rate. Moreover, our analysis suggests that the consideration of nonimpulsive labelling might improve the estimation of the kinetic parameters of the experimental tumour. In this paper we have no longer pursued this last point, in view of the difficulties of the estimation problem, since we think that a larger set of experimental data with a better statistics be necessary to reliably determine the characteristics of the labelling.

Finally, we notice that an improved assessment of the kinetic heterogeneity should also consider phenomena that were neglected in the present model, such as the arrest of the progression of cell in S and G2M phases (White, 1991) and the possibility that dead cells in early stages after death are measured with unchanged levels of red and green fluorescences.

Appendix A

The fractions of S and G2M cells in AEG, f_S and f_{G2M} respectively, are given by

$$f_S = \int_{T'}^{T''} \int_0^{T_S(T)} \nu(a,T)\, da dT\,, \quad f_{G2M} = \int_{T'}^{T''} \int_{T_S(T)}^{T} \nu(a,T)\, da dT\,.$$

From equation (13) we easily get

$$f_S = \int_{T'}^{T''} p_T(T)(\mathrm{e}^{\beta T} - \mathrm{e}^{\beta T_{G2M}(T)})\, dT \tag{A.1}$$

$$f_{G2M} = \int_{T'}^{T''} p_T(T)(\mathrm{e}^{\beta T_{G2M}(T)} - 1)\, dT \tag{A.2}$$

By expanding the exponentials up to the second order, we obtain the following approximate expressions for the phase fractions:

$$f_S \simeq \beta\langle T_S(T)\rangle + \frac{\beta^2}{2}[\langle T\rangle^2 + \mathrm{SD}(T)^2 - \langle T_{G2M}(T)\rangle^2 - \mathrm{SD}(T_{G2M})^2] \tag{A.3}$$

$$f_{G2M} \simeq \beta\langle T_{G2M}(T)\rangle + \frac{\beta^2}{2}[\langle T_{G2M}(T)\rangle^2 + \mathrm{SD}(T_{G2M})^2]\,, \tag{A.4}$$

where $\langle\cdot\rangle$ denotes the mean and $\mathrm{SD}(\cdot)$ denotes the standard deviation. By the same approximation, the fraction of cells in compartment 1, given by (16), can be written as

$$f_1 = 1 - \beta\langle T\rangle - \frac{\beta^2}{2}[\langle T\rangle^2 + \mathrm{SD}(T)^2]\,. \tag{A.5}$$

Note that the sum of the above approximated fractions is equal to 1.

Appendix B

Two cases have to be distinguished, depending on whether T' is smaller or larger than $(1-\gamma)T''$. In the first case the time $\bar{t}=(1-\gamma)T''$ is greater than T' and we have:

$$f^{lu}(t) = \begin{cases} f_S \mathrm{e}^{-\beta t}, & 0<t\le(1-\gamma)T' \\ (2-f_1)\mathrm{e}^{-\beta t} - \int_{T'}^{t/(1-\gamma)} p_T(T)\, dT - \mathrm{e}^{-\beta t}\int_{t/(1-\gamma)}^{T''} p_T(T)\mathrm{e}^{\beta(1-\gamma)T}\, dT, & (1-\gamma)T'\le t<T' \\ \mathrm{e}^{-\beta t}\int_t^{T''} p_T(T)\mathrm{e}^{\beta T}\, dT - \int_t^{t/(1-\gamma)} p_T(T)\, dT - \mathrm{e}^{-\beta t}\int_{t/(1-\gamma)}^{T''} p_T(T)\mathrm{e}^{\beta(1-\gamma)T}\, dT, & T'<t\le\bar{t} \\ \mathrm{e}^{-\beta t}\int_t^{T''} p_T(T)\mathrm{e}^{\beta T}\, dT - \int_t^{T''} p_T(T)\, dT, & \bar{t}<t\le T''\,. \end{cases} \tag{B.1}$$

In the second case $\bar{t}$ is smaller than T' and we have:

$$f^{lu}(t) = \begin{cases} f_S \mathrm{e}^{-\beta t}, & 0<t\le(1-\gamma)T' \\ (2-f_1)\mathrm{e}^{-\beta t} - \int_{T'}^{t/(1-\gamma)} p_T(T)\, dT - \mathrm{e}^{-\beta t}\int_{t/(1-\gamma)}^{T''} p_T(T)\mathrm{e}^{\beta(1-\gamma)T}\, dT, & (1-\gamma)T'\le t<\bar{t} \\ (2-f_1)\mathrm{e}^{-\beta t} - 1, & \bar{t}<t\le T' \\ \mathrm{e}^{-\beta t}\int_t^{T''} p_T(T)\mathrm{e}^{\beta T}\, dT - \int_t^{T''} p_T(T)\, dT, & T'<t\le T''\,. \end{cases} \tag{B.2}$$

Appendix C

We assume, for the rate of DNA synthesis with respect to the DNA content x, a downward concave parabolic function having the maximum at $\bar{x} \in (1,2)$ and the value at $x=1$ equal to a fraction k, $k<1$, of the maximum. For simplicity, we consider first the case of cells having the same S-phase duration T_S, so we omit the argument T. Denoting by c the maximum of the DNA synthesis rate $w(x)$, we have

$$w(x) = c\left[1 - \frac{1-k}{(\bar{x}-1)^2}(x-\bar{x})^2\right], \quad x \in [1,2]\,.$$

The value of c will depend on the value of T_S according to

$$T_S = \int_1^2 \frac{dx}{w(x)}\,,$$

so that, computing the integral in the above equation, we obtain

$$w(x) = \frac{1}{T_S}\,\frac{(\bar{x}-1)\,\varphi}{2\sqrt{1-k}}\left[1 - \frac{1-k}{(\bar{x}-1)^2}(x-\bar{x})^2\right], \tag{C.1}$$

where

$$\varphi = \log\left(\frac{\bar{x}-1+(2-\bar{x})\sqrt{1-k}}{\bar{x}-1-(2-\bar{x})\sqrt{1-k}}\,\frac{1+\sqrt{1-k}}{1-\sqrt{1-k}}\right). \tag{C.2}$$

The age of a cell with DNA content x, $a(x)$, is given by

$$a(x) = \int_1^x \frac{dz}{w(z)}$$

$$= \frac{T_S}{\varphi}\log\left(\frac{\bar{x}-1+(x-\bar{x})\sqrt{1-k}}{\bar{x}-1-(x-\bar{x})\sqrt{1-k}}\,\frac{1+\sqrt{1-k}}{1-\sqrt{1-k}}\right). \tag{C.3}$$

By inverting (C.3), we obtain the DNA content as a function of the age in S by means of

$$x(a) = \frac{\gamma(a)-1}{\gamma(a)+1}\,\frac{\bar{x}-1}{\sqrt{1-k}} + \bar{x} \tag{C.4}$$

with

$$\gamma(a) = \frac{1-\sqrt{1-k}}{1+\sqrt{1-k}}\exp\big(\frac{\varphi}{T_S}\,a\big)\,. \tag{C.5}$$

By differentiating $x(a)$ with respect to a, we express the DNA synthesis rate as a function of the age, $v(a)$, as

$$v(a) = \frac{\varphi(\bar{x}-1)}{T_S\sqrt{1-k}}\,\frac{2\gamma(a)}{(\gamma(a)+1)^2}\,. \tag{C.6}$$

In the case of distributed transit time in S, according to the present model, we have to take into account that it is $T_S = T_S(T)$, thus obtaining the functions $w(x,T)$, $a(x,T)$ and $v(a,T)$ for cells of class T.

References

Bagwell, C.B. (1993). Theoretical aspects of flow cytometry data analysis, in *Clinical Flow Cytometry*, K.D. Bauer, R.E. Duque and T.V. Shankey (Eds.), Baltimore, Williams and Wilkins, pp. 41-61.

Baisch, H. and U. Otto (1993). Intratumoral heterogeneity of S phase transition in solid tumours determined by bromodeoxyuridine labelling and flow cytometry. *Cell Prolif.* **26**, 439-448.

Baisch, H., U. Otto, U. Hatje and H. Fack (1995). Heterogeneous cell kinetics in tumors analyzed with a simulation model for bromodeoxyuridine single and multiple labeling. *Cytometry* **21**, 52-61.

Begg, A.C., N.J. McNally, D.C. Shrieve and H. Kärcher (1985). A method to measure the duration of DNA synthesis and the potential doubling time from a single sample. *Cytometry* **6**, 620-626.

Bergers, E., P.J. van Diest and J.P. Baak (1996). Tumour heterogeneity of DNA cell cycle variables in breast cancer measured by flow cytometry. *J. Clin. Pathol.* **49**, 931-937.

Bertuzzi, A., N. Del Grosso, A. Gandolfi, C. Sinisgalli and G. Starace (1995a). Cell cycle analysis by the relative movement approach: effect of variability across S-phase of DNA synthesis rate. *Cell Prolif.* **28**, 107-120.

Bertuzzi, A., A. Gandolfi, C. Sinisgalli and G. Starace (1995b). Relationship between DNA synthesis rate and DNA-BrdUrd distribution in pulse labelling experiments, in *Mathematical Population Dynamics: Analysis of Heterogeneity, Vol. 2*, O. Arino, D. Axelrod and M. Kimmel (Eds.), Winnipeg: Wuerz, pp. 71-86.

Bertuzzi, A. and A. Gandolfi (1997). Some results on the determination of cell kinetic parameters from DNA-BrdUrd measurements. *Studi Urbinati, Serie A* **1**, 169-179.

Bertuzzi, A., A. Gandolfi, C. Sinisgalli and G. Starace (1997). Estimation of cell cycle kinetic parameters by flow cytometry, in *Advances in Mathematical Population Dynamics - Molecules, Cells and Man*, O. Arino, D. Axelrod and M. Kimmel (Eds.), Singapore: World Scientific, pp. 167-180.

Bertuzzi, A. and A. Gandolfi (1999). A model for estimating cell kinetic parameters of experimental tumours studied by BrdUrd labelling and flow cytometry. *Arch. Control Sci.* **9**, 41-56.

Carlton, J.C., N.H.A. Terry and R.A. White (1991). Measuring potential doubling times of murine tumors using flow cytometry. *Cytometry* **12**, 645-650.

Chiorino, G., J.A.J. Metz, D. Tomasoni and P. Ubezio (2001). Desynchronization rate in cell populations: mathematical modeling and experimental data. *J. theor. Biol.*, in press.

Dolbeare, F., H. Gratzner, M.G. Pallavicini and J.W. Gray (1983). Flow cytometric measurement of total DNA content and incorporated bromodeoxyuridine. *Proc. Nat. Acad. Sci. USA* **80** 5573-5577.

Dolbeare, F. (1995). Bromodeoxyuridine: a diagnostic tool in biology and medicine, Part I: historical perspectives, histochemical methods and cell kinetics. *Histochem. J.* **27**, 339-369.

Gratzner, H.G. (1982). Monoclonal antibody to 5-bromo- and 5-iododeoxyuridine: a new reagent for detection of DNA replication. *Science* **218**, 474-475.

Kallinowski, F., K.H. Schlenger, S. Runkel, M. Kloes, M. Stohrer, P. Okunieff and P. Vaupel (1989). Blood flow, metabolism, cellular microenvironment, and growth rate of human tumor xenografts. *Cancer Res.* **49**, 3759-3764.

Kriss, J.P. and L. Revesz (1961). Quantitative studies of incorporation of exogenous thymidine and 5-bromodeoxyuridine into deoxyribonucleic acid of mammalian cells in vitro *Cancer Res.* **21**, 1141-1147.

Massazza, G., A. Tomasoni, A. Lucchini, P. Allavena, E. Erba, N. Colombo, A. Mantovani, M. D'Incalci, C. Mangioni and R. Giavazzi (1989). Intraperitoneal and subcoutaneous xenograft of human ovarian carcinoma in nude mice and their potential in experimental therapy. *Int. J. Cancer* **44**, 494-500.

Powell, B.L., B.W. Gregory, T.E. Kute, T.M. Morgan, E.S. Lyerly and R.L. Capizzi (1990). Bromodeoxyuridine incorporation into DNA of human leukemia cells is not concentration dependent. *Cytometry* **11**, 438-441.

Sisken, J.E. and L. Morasca (1965). Intrapopulation kinetics of the mitotic cycle. *J. Cell Biol.* **25**, 179-189.

Steel, G.G. (1977). *Growth Kinetics of Tumours: Cell Population Kinetics in Relation to the Growth and Treatment of Cancer*, Oxford: Clarendon Press.

Terry, M.H.A., C.G. Milross, N. Patel, K.A. Mason, R.A. White and L. Milas (1997). The effect of paclitaxel on the cell cycle kinetics of a murine mammary adenocarcinoma in vivo. *Breast J.* **3**, 99-105.

Ubezio, P. (1990). Cell cycle simulation for flow cytometry, *Comp. Meth. Programs Biomed.* **31**, 255-266.

Ubezio, P. S. Filippeschi and L. Spinelli (1991). Method for kinetic analysis of drug-induced cell cycle perturbations. *Cytometry* **12**, 119-126.

White, R.A. and M.L. Meistrich (1986). A comment on "A method to measure the duration of DNA synthesis and the potential doubling time from a single sample". *Cytometry* **7**, 486-490.

White, R.A. (1989). Computing multiple cell kinetic properties from a single time point. *J. theor. Biol.* **141**, 429-446.

White, R.A., N.H.A. Terry and M.L. Meistrich (1990). New methods for calculating kinetic properties of cells in vitro using pulse labelling with bromodeoxyuridine. *Cell Tissue Kinet.* **23**, 561-573.

White, R.A. (1991). A theory for analysis of cell populations with non-cycling S phase cells. *J. Theor. Biol.* **150**, 201-214.

White, R.A., M.L. Meistrich, A. Pollack and N.H. Terry (2000). Simultaneous estimation of T(G2+M), T(S), and T(pot) using single sample dynamic tumor data from bivariate DNA-thymidine analogue cytometry. *Cytometry* **41**, 1-8.

Yanagisawa, M., F. Dolbeare, T. Todoroki and J.W. Gray (1985). Cell cycle analysis using numerical simulation of bivarite DNA/Bromodeoxyuridine distributions. *Cytometry* **6**, 550-562.